

## Multi objective design optimization of plate fin heat sinks using improved differential search algorithm

Oguz Emrah TURGUT\*<sup>1</sup>

Accepted : 13/07/2017 Published: 30/03/2018

**Abstract:** This study provides the multi-objective optimization of plate fin heat sinks equipped with flow – through and impingement-flow air-cooling system by using Improved Differential Search algorithm. Differential Search algorithm mimics the subsistence characteristics of the living beings through the migration process. Convergence speed of the algorithm is enhanced with the local search based perturbation schemes and this improvement yields favorable solution outputs according to the results obtained from the widely quoted optimization test problems. Improved algorithm is employed on multi-objective design optimization of plate fins heat sink considering the objective functions of entropy generation rate and total material cost. Total of seven decision variables such as oncoming stream velocity, number of fins on the plate, gap between consecutive fins, base thickness of the plate, width, length and height of the plate fin heat sink are selected to be optimized. Pareto frontiers are constructed for both flow-through and impingement flow air-cooling system design and best solutions are obtained by means of widely reputed decision-making theories of LINMAP, TOPSIS, and Shannon’s entropy theory. Results retrieved from the case studies show that reliable outcomes could be achieved in terms of solution accuracy through Improved Differential Search optimizer.

**Keywords:** Decision making, Differential Search, Metaheuristic algorithms, Multi objective optimization, Plate fin heat sink

### Introduction

Heat sinks are the essential and indispensable components of the devices, which dissipate the generated heat inside the high-tech tools [1]. They are passive heat carriers working with highly powered semi-conductor devices. There are several design parameters including air velocity, choice of material and protrusion design that affect the heat removal performance of the heat sinks. Application of a heat sink on the state-of-art technologies having a high amount of heat load is found to be the effective and efficient considering the imposed cost, weight, and space constraints [2]. In order to achieve successful design, a designer should maintain a plausible temperature gradient between heat sink and ambient that paves the way for the long-term reliability of the electronic component. Component in hand involves resistive paths as heat flows through the circuited boards to the surroundings. Among the various types of resistance layers on the electronic package, boundary layer resistance is the dominant and controlling resistance that directly effects on the overall heat removal process [3]. Film (boundary layer) resistance is under the control of convective heat transfer coefficient and total surface area. Considering this behavior, a designer should increase heat transfer coefficient, total heat transfer area or both of them if it is to procure a reduction in fin resistance rates. Velocity increase around the heat sink results in a significant rise in heat transfer rates however, this increase is restricted to some extent due to the operational and constructional constraints. Another suitable alternative, increasing the total heat transfer area, can be maintained by using heat sinks or extended surfaces.

Literature is composed of many theoretical and experimental studies concerning the optimal thermal design of the heat sinks. Sparrow et al. [4] concluded a research, which investigates the solution of the velocity field occurred in the space between consecutive fins. After comprehensive parametrical studies, it was found that usage of traditional heat transfer coefficient model in plate fin heat sink design may lead to unexpected and

unsatisfactory results. Goldberg [5] proposed a correlation for obtaining favorable plate fin design conditions under constant air flow rates. Knight et al. [6,7] presented an optimization procedure to reduce the thermal resistance and increase the efficiency of the heat dissipation. They proposed a mathematical model to determine the effect of the fin shape on the total heat removal process. Bejan [8] proposed entropy generation rate as a novel way to design optimal fin geometry and asserted that a designer can simultaneously minimize total heat transfer area and convective heat transfer coefficient by utilizing this method. Several researchers have used this propounded strategy to optimize heat sink geometry. For instance, Khan et al.[9] used entropy generation minimization as a measure to investigate the thermodynamic losses occurred in cylindrical pin-fin heat sinks. Lagrange multiplier method is applied to optimize given set of design variables. Ndao et al.[10] applied multi objective genetic algorithm to accomplish the thermal design of cooling technologies. They put forward total thermal resistance and pumping power consumption as objective functions to be minimized, thereby plotting a Pareto frontier to determine to trade-off solutions between conflicting objectives. Iyengar and Bar-Cohen [11] presented coefficient of performance analysis for plate fin heat sinks in the effect of the force convection and concluded that entropy generation minimization methodology is viable procedure to obtain least-material cost. Bejan and Morega [12] proposed a methodology to attain optimal geometry for round pin fins and staggered parallel-plate fins based on the concurrent minimization of thermal resistance between the conjunction layers and forced flow through the fins. Chen and Chen [1] took into consideration of entropy generation minimization and total cost as contradictory design objectives so as to capture optimum trade-off solutions through multi-objective real-coded genetic algorithm. Genetic algorithm was applied for multi objective design optimization of a micro heat sink for Concentrating Photovoltaic/Thermal (CPVT) systems. Fixed and stepwise variable width microchannel configurations are considered for optimum arrangement and results showed that microchannel heat sinks can achieve considerably low values of thermal resistance [13]. Baby and Balaji [14] proposed a hybrid artificial neural network – genetic algorithm to determine the optimum

<sup>1</sup> Ege University, Department of Mechanical Engineering, 35040, Izmir, TURKEY

\* Corresponding Author: Email: oeturgut@hotmail.com

configuration of phase change material pin fin heat sink, which maximizes the operating time. Kim [15] utilized volume-averaging theory to optimize thermal performance of the vertical plate fin heat sink in the effect of natural convection as the thickness of the fin varies across the flow direction. Soleimani et al. [16] used Particle Swarm Optimization algorithm to determine the optimum positions of a pair heat source-sink in an enclosure by minimizing the maximum temperature on the heat source under a constant heat flux. Numerical results confirmed that optimum position of heat source varies with increasing Rayleigh number. Rao and Waghmare [17] considered teaching learning based optimization for multi-objective design of a plate fin heat sink under the effect of flow through and impingement-flow air-cooling systems. Entropy generation minimization and overall material cost accompanied with several design constraints were selected as conflicting objectives to be concurrently optimized. Number of fins along the flow direction, gap between two consecutive fins, height of the fins and air velocity were modeled as design variables. Optimization results revealed that proposed method found better solutions than those of the previous studies available in the literature. A brief overview of heat sink optimization literature is mentioned in Table 1.

**Table 1.** A brief literature overview of heat sink optimization

| Ref  | Description                                                                                                                                                                                                                    |
|------|--------------------------------------------------------------------------------------------------------------------------------------------------------------------------------------------------------------------------------|
| [1]  | Genetic Algorithm is applied to multi-objective micro heat sink optimization problem to find the minimum of entropy generation and total cost.                                                                                 |
| [8]  | Entropy generation rate is utilized to find the optimum fin geometry.                                                                                                                                                          |
| [12] | A methodology is proposed to find optimal geometry round pin fins and staggered parallel-plate fins based on the concurrent minimization of thermal resistance between the conjunction layers and forced flow through the fins |
| [14] | A hybrid artificial neural network - genetic algorithm is proposed to calculate the optimum configuration of phase change material pin fin heat sink.                                                                          |
| [15] | Volume averaging theory is applied to optimize the performance of vertical plate fin heat sink.                                                                                                                                |
| [16] | Particle Swarm Optimization algorithm is used to determine the optimal position of a pair heat source-sink by minimizing the maximum temperature on the heat source.                                                           |
| [17] | Teaching Learning Based Optimization algorithm is utilized for multiobjective design optimization of a plate-fin heat sink. The objectives were selected as entropy generation and material cost.                              |

Literature studies showed that there is still room to improve the existing optimization and design methodologies in order to obtain more accurate solutions. Most of the available literature approaches have used limited optimization variables, which restrict the best results in a narrow solution space. Moreover, majority of the existing studies have applied parametric optimization methods instead of traditional optimization algorithms. As stated in [1], optimal heat sink design is generally based on minimum entropy generation, which forces the designer to model larger size of heat sink. In this study, in order to attain a balanced solution between conflicting objectives, an improved version of Differential Search (DS) algorithm is practiced to obtain optimal design variables of plate fin heat sinks equipped with several imposed design constraints. Differential Search [18-21] algorithm is a recently developed novel metaheuristic optimization method, which is constructed on the migration behaviors of the individuals when their food resources are depleted in a habitat. Since proposed algorithm does not contain algorithm specific parameters, it avoids tedious parameter tuning process which makes the application of the propounded DS more simpler than any other optimizer whose accuracy is controlled by the efficient tuning of algorithm parameters. With utilizing the proposed design framework, it is intended to compare the heat emission capacity of the plane-heat sinks supplied with flow-

through and impingement-flow air systems. The remainder of the paper is formatted as follows: Section 2 gives the formulation of the plate-fin heat sinks configured with impingement-flow and flow-through air systems. Section 3 explains the fundamentals of Differential Search algorithm and improvements made on the algorithm at hand. Efficiency of the proposed optimizer is tested on the widely quoted optimization test functions. Following that, the design problem dealing with the concurrent minimization of entropy generation rate and the total material cost is solved by the improved Differential Search algorithm and sensitivity analysis on the design variables of the models are conducted. Finally, the paper is concluded with the remarkable comments in Section 4.

## Problem Description

Effectivity and accuracy of the proposed improved Differential Search algorithm will be assessed by testing it on the heat sink design problem having with flow-through and impingement-flow system as depicted in Fig.1(a-b). In order to make simplifications on the design process, following assumptions are made while modelling heat sink systems with flow-through and impingement – flow air cooling systems [1,17]

- No spreading or constriction resistance,
- No contact resistance between the mounted heat sink and the base device,
- Uniform and constant heat convection coefficients,
- No bypassing air flow,
- Adiabatic condition on the fin tip,
- Uniform oncoming air velocity,
- Incompressible and laminar air flow and constant physical properties and the heat generated in the device are uniformly distributed,

In order to make thermal analysis related to plate fin heat sinks under the effect of forced flow conditions, following mathematical model of entropy generation rate developed by Bejan [22] is put into practice.

$$\dot{S}_{gen} = \left( \frac{\dot{Q}}{T_{amb}} \right)^2 R_{sink} + \frac{F_d V_f}{T_{amb}} \quad (1)$$

Where  $\dot{Q}$  stands for the heat generation rate,  $T_{amb}$  is the ambient temperature,  $F_d$  represents the air resistance between fins and  $V_f$  symbolizes the oncoming air velocity. As it is observed in Eq.(1), entropy generation rate is dependent of total heat resistance  $R_{sink}$ . Eq. (2) gives the formulation of the total heat resistance for both flow-through and impingement-flow air cooling systems [23]

$$R_{sink} = \begin{cases} \frac{1}{\left( N / R_{fin} \right) + h_{eff} (N-1) bL} + \frac{t_b}{kLW}, & \text{for flow - through configuration} \\ \frac{1}{h_{eff} A \eta_{fin}}, & \text{for impingement - flow configuration} \end{cases} \quad (2)$$

Where  $b$  is the gap between fins and shown as

$$b = \frac{W - t_w}{N - 1} - t_w \quad (3)$$

Eq. (2),  $N$  denotes the number of fins,  $A$  is the total surface area that inherits fins and other exposed surfaces, and  $\eta_{fin}$  represents heat dissipation efficiency formulated by the following equation [12].

$$\eta_{fin} = \frac{\tanh(mH)}{mH} \quad (4)$$

Heat resistance related to flow-through air-cooling system can be attained as follows [20]:

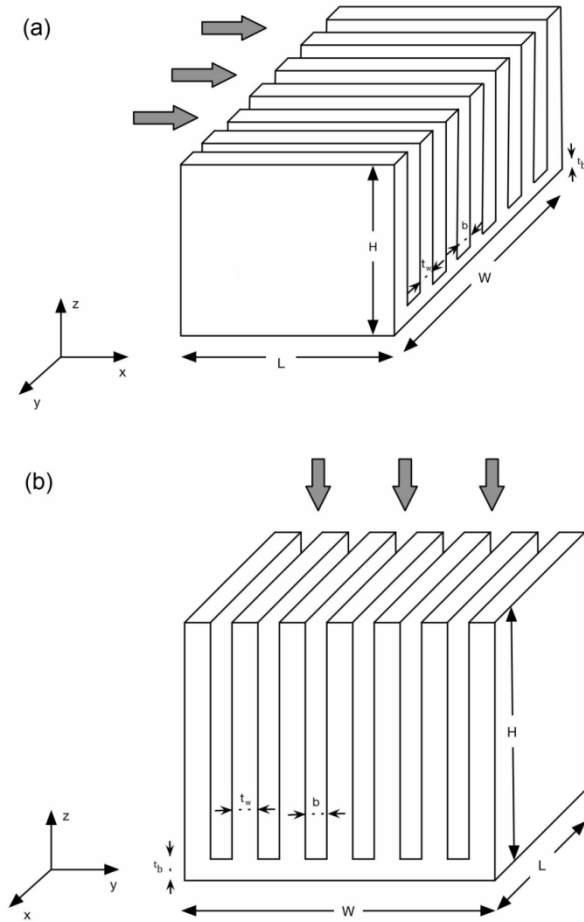


**Figure 1.** (a) Plate fin heat sink equipped with flow through air cooling system (b) Plate fin heat sink equipped with impingement flow air cooling system

$$R_{fin} = \frac{1}{\sqrt{h_{eff} P k A_c} \tanh(mH)} \quad (5)$$

Where

$$m = \sqrt{\frac{h_{eff} P}{k A_c}} \quad (6)$$

Above the Eqs. (5) and (6),  $P$  and  $A_c$  correspondingly denote the perimeter and cross-sectional area of each fin. Taking into account of the total force balance on the heat fin sink, total drag force between fins can be calculated by Kays and London [20].

$$F_d = \left(0.5 \rho V_{ch}^2\right) f_{app} N (2HL + bL) + K_c (HW) + K_e (HW) \quad (7)$$

Where  $F_d$  is the drag force,  $f_{app}$  is the friction coefficient,  $K_c$  and  $K_e$  are the sudden expansion and contraction coefficients, correspondingly. Velocity of the air,  $V_{ch}$ , flowing through in the channel for impingement-flow and flow-through air cooling systems can be formulated by Muzychka and Yovanovich [24].

$$V_{ch} = \begin{cases} V_f \left(1 + \frac{t_w}{b}\right), & \text{for flow-through configuration} \\ \frac{V_f L}{2H}, & \text{for impingement-flow configuration} \end{cases} \quad (8)$$

The friction coefficient ( $f_{app}$ ) term in Eq.(7) is calculated by the following equation [24]

$$f_{app} Re_{Dh} = \sqrt{\left(\frac{3.44}{\sqrt{L^*}}\right)^2 + (f Re_{Dh})^2} \quad (9)$$

Where  $L^* = L / (D_h Re_{Dh})$  and  $D_h$  is the hydraulic diameter of the related channel. Reynold number group, denoting the friction factor for fully developed flow, is represented by Muzychka and Yovanovich [24]

$$f Re_{Dh} = 24 - 32.527 \left(\frac{b}{H}\right) + 46.271 \left(\frac{b}{H}\right)^2 - 40.829 \left(\frac{b}{H}\right)^3 + 22.954 \left(\frac{b}{H}\right)^4 - 6.089 \left(\frac{b}{H}\right)^5 \quad (10)$$

Calculation of the sudden contraction and expansion coefficients can be explained by the following relations [25]

$$K_c = 0.42 (1 - \sigma^2) \quad (11)$$

$$K_e = (1 - \sigma^2)^2 \quad (12)$$

Where

$$\sigma = 1 - \frac{Nt_w}{W} \quad (13)$$

Convective heat transfer coefficient is obtained by the following equation [26].

$$Nu_b = \left[ \left( \frac{Re_b^* Pr}{2} \right)^{-3} + \left( 0.664 \sqrt{Re_b^* Pr}^{1/3} \sqrt{1 + \frac{3.65}{\sqrt{Re_b^*}}} \right)^{-3} \right]^{-0.333} \quad (14)$$

Where  $Pr$  stands for the Prandtl number

$$Nu_b = h_{eff} b / k_f \quad (15)$$

$$Re_b^* = Re_b (b / L) \quad (16)$$

$$Re_b = V_{ch} b / \nu \quad (17)$$

Finally, the multi objective plate fin heat sink design problem is formulated as the following relation [17].

$$\arg \min = \left\{ \dot{S}_{gen}, C_{mat} \right\} \quad (18)$$

Where  $\dot{S}_{gen}$  is the entropy generation rate as given in Eq.(1) and the total cost of the plate fin heat sink is represented by

$$C_{mat} = (W \cdot L \cdot t_{bp} + N \cdot H \cdot t_w \cdot L) \cdot \rho_m \cdot \text{Price}_{Al} \quad (19)$$

Where  $C_{mat}$  is total material cost of the plate fin heat sink;  $\text{Price}_{Al}$  is the price of the aluminum which heat sink is made of;  $W, L$  and  $H$  are respectively width, length and height of the plate fin heat sink,  $t_{bp}$  is the base length of the fin,  $t$  is the thickness of the fin, and  $\rho_m$  is the density of the material. On the course of minimizing these two conflicting objectives, below given geometry constraints should be satisfied.

$$G_1 : 0.001 - b \leq 0 \quad (20)$$

$$G_2 : b - 0.005 \leq 0 \quad (21)$$

$$G_3 : 0.01 - \frac{H}{b} \leq 0 \quad (22)$$

$$G_4 : \frac{H}{b} - 19.4 \leq 0 \quad (23)$$

$$G_5 : 0.0001 - \sqrt{\frac{b \cdot V_{ch}}{v} \cdot \frac{b}{L}} \leq 0 \quad (24)$$

In the constraints given above,  $G_1$  and  $G_2$  confirm that the gap between consecutive fins should be in between 0.001 and 0.005 m. Satisfaction of the constraints  $G_3$  and  $G_4$  maintain large design space for installation. If it is to explain in a more specific manner, these two constraints aim to fit the ratio of the height to thickness of the fin in between 0.01 and 19.4 due to the limited space for installation. Constraint  $G_5$  is practiced to eliminate the divide-by-zero error of  $Re_b^*$ . Moreover, following design constraints' should also be applied in order for acquire feasible solutions within the search space:

$$40.0 \text{ mm} \leq W \leq 60.0 \text{ mm}, 40.0 \text{ mm} \leq L \leq 60.0 \text{ mm}, 2 \leq N \leq 40,$$

$$0.025 \text{ m} \leq H \leq 0.14 \text{ m}, 2 \times 10^{-4} \text{ m} \leq t_w \leq 2.5 \times 10^{-4} \text{ m},$$

$$0.5 \text{ m/s} \leq V_f \leq 2.0 \text{ m/s} \text{ and } N \times b \leq 0.05 \text{ m}.$$

As it was stated by several researchers in the literature, these two conflicting objectives should be minimized simultaneously in order to obtain pareto solutions which takes into account of above given imposed constraints to circumvent the violated solutions. In this paper, it is aimed to give relations between decision variables and objective functions as well as trade-off solutions between objectives. For instance, any increase of the heat sink length and width gives rise to the total cost whilst concluding a remarkable decrease in entropy generation rates. Parametric evaluations on design variables will be executed to observe the variations in objective function values. Decision making methods including LINMAP, TOPSIS and Shannon's entropy theory will also be applied to decide the optimum trade-off solutions on the pareto curve.

## Differential Search Algorithm

### 3.1. Fundamentals of Differential Search Algorithm

Especially designed for multi-dimensional optimization problems by Civicioglu [18], Differential Search is a derivative free metaheuristic algorithm based on the migration behavior of the living beings. Algorithm simulates the Brownian-like random-

walk movement on the course of migration process to probe more fruitful habitat locations. Inspired by the population-based metaheuristics[27,29] available in the literature, algorithm is constructed on decision making process of the individuals which are moving away from their current habitat due to depleted food resources. Migration is in the control of a superorganism formed by individuals and decided by the fertility and productivity of the migrated areas. Superorganism probes around the possible locations in the search space and makes its way towards the more fruitful habitat. In other saying, if the current living space meets the needs of the superorganism then superorganism has rights to stay there for a period of time. Otherwise, superorganism tends to migrate to another location.

In the context of Differential Search Algorithm, like the other population based optimization algorithms, algorithm is initiated by forming of artificial superorganism which consists of randomly generated D-dimensional decision variables restricted between upper and lower bounds of the search space. Arbitrary artificial superorganism is initiated by  $X_i=[x_{ij}]$ , where  $x_{ij}$  are the individuals of the D-dimensional objective function. An artificial superorganism consists of N artificial organisms, denoted by  $\text{Superorganism}_g=[X_i]$  where  $i=\{1,2,3,\dots,N\}$  and  $g$  is the  $g^{\text{th}}$  generation ( $g=1,2,3,\dots,\text{maxgeneration}$ ). In DS algorithm concept, probing mechanism of productive areas, stopover sites, is sustained by Brownian-like random walk model [29]. Individuals selected randomly from the superorganism moves towards the donor targets ( $[X_{\text{random\_shuffling}(i)}]$ ) so as to reach fertile stopoversites. Proposed perturbation scheme shuffles the order of the elements in the set  $i=\{1,2,3,\dots,N\}$  and the mentioned shuffling process is carried out under the control of scale value which is produced by utilizing gamma-random number generator. Determination of the position of the stopover sites is calculated by the following equation

$$\text{Stopoversite} = \text{Superorganism} + \text{Scale} \times (\text{donor} - \text{Superorganism}) \quad (25)$$

If the condition of a stopover site target is more fertile than that of the current one, individuals of the artificial superorganism tends to move to the stopover site. The search for global optimum is controlled by this iterative food resource seeking mechanism and algorithm halts the ongoing process until maximum number of generation is reached. Structural mathematical representation of the randomized iterative fertile area search mechanism is described lines between 8 - 29 in Table 2. If any of the perturbed solution vector goes beyond the upper and lower limits of the habitat (search space), algorithm pushes it into another suitable position in the habitat. DS has only two algorithm specific control parameters (i.e.  $p_1$  and  $p_2$ ) which can be taken  $p_1=0.3$  and  $p_2=0.3$  as suggested by Civicioglu [18]. Pseudo-code of the proposed Differential Search algorithm is given in Table 2.

### 3.2. Improvements on Differential Search Algorithm

Metaheuristic algorithms are generally known as efficient problem solvers those having the ability of producing acceptable solutions in a reasonable time by using trial-and-error methodology. In the context of metaheuristics, there is no guarantee in finding the global optimum solution even if the maximum number of iteration is reached. Emerging technologies in the world makes engineering design problems more complex and exhaustive therefore, in structural design optimization point of view, it becomes nearly impossible to visit every possible solution or combination in the search space. Among the solutions obtained on the course of iterations, some of them are nearly optimal due to the complexity of the problem as well as the diversity of the solution space. Metaheuristic algorithms have two major components. These are intensification (exploration) and diversification (exploitation) [30]. Diversification increases the solution diversity by making extensive exploration on the search space while intensification

focuses on the local promising solutions obtained after diversification process in order to exploit the information, which paves the way for better results. Diversification decreases the

convergence speed of the algorithm through tedious perturbation schemes while leading to maintain solutions that are more diverse.

**Table 2.** Pseudo code of Differential Search Algorithm [18]

**Algorithm : Differential Search Algorithm**

---

N : The size of the population, where  $i=\{1,2,3,\dots,N\}$   
D : The dimension of the problem  
G : Maximum number of generation  
1:  $Superorganism = initialize()$ , where  $Superorganism = [ArtificialOrganism_i]$   
2:  $y_i = Evaluate (ArtificialOrganism_i)$   
3: **for** cycle 1:G **do**  
4:      $donor = Superorganism_{Random\_Shuffling(i)}$   
5:      $Scale = randg[2 \cdot rand_1] \cdot (rand_2 - rand_3)$   
6:      $StopoverSite = Superorganism + Scale \cdot (donor - Superorganism)$   
7:      $p_1 = 0.3 \cdot rand_4$  and  $p_2 = 0.3 \cdot rand_5$   
8:     **if**  $rand_6 < rand_7$  **then**  
9:         **if**  $rand_8 < p_1$  **then**  
10:              $r = rand(N, D)$   
11:             **for** Counter1 = 1 : N **do**  
12:                  $r(Counter1,:) = r(Counter,:)$   $< rand_9$   
13:             **endfor**  
14:             **else**  
15:                  $r = ones(N, D)$   
16:                 **for** Counter2 = 1 : N **do**  
17:                      $r(Counter2, randi(D)) = r(Counter2, randi(D)) < rand_{10}$   
18:                 **endfor**  
19:             **endif**  
20:         **else**  
21:              $r = ones(N, D)$   
22:             **for** Counter3 = 1 : N **do**  
23:                  $d = randi(D, 1, \lceil p_2 \cdot rand \cdot D \rceil)$   
24:                 **for** Counter4 = 1 : size(d) **do**  
25:                      $r(Counter3, d(Counter4)) = 0$   
26:                 **endfor**  
27:             **endfor**  
28:         **endif**  
29:          $individuals_{I,J} \leftarrow r_{I,J} > 0 \mid I \in i, J \in [1, D]$   
30:          $StopoverSite(individuals_{I,J}) := Superorganism(individuals_{I,J})$   
31:         **if**  $StopoverSite_{i,j} < low_{i,j}$  or  $StopoverSite_{i,j} > up_{i,j}$  **then**  
32:              $StopoverSite_{i,j} := rand \cdot (up_j - low_j) + low_j$   
33:         **endif**  
34:          $y_{StopoverSite(i)} = Evaluate(StopoverSite_i)$   
35:          $y_{Superorganism(i)} := \begin{cases} y_{StopoverSite(i)} & \text{If } y_{StopoverSite(i)} < y_{Superorganism(i)} \\ y_{Superorganism(i)} & \text{else} \end{cases}$   
36:          $ArtificialOrganism_i := \begin{cases} StopoverSite_i & \text{If } y_{StopoverSite(i)} < y_{Superorganism(i)} \\ ArtificialOrganism_i & \text{else} \end{cases}$   
37:     **endfor**

---

On the other hand, a rapid convergence can be attained by intensification phase however, algorithm could be trapped in local optimum points in the search space. Therefore, it can be concluded that an agreeable balance between diversification and intensification shapes the characteristics of the metaheuristics in a positive way and gives rise to obtain more accurate solutions. In DS algorithm, diversification phase is carried out by Brownian-like random walks as it is described the lines between 8 and 28 in Table 2. Exploitation of promising solutions is maintained by the greedy selection mechanism as shown the lines between 35 and 36 in Table 2.

From the numerical experiments, it is observed that DS algorithm suffers from the late convergence and immature solutions due the extensive appliance of global search based perturbation schemes. In addition, it is seen that local search mechanism, by which convergence rate of the algorithm is enhanced, takes a limited role on the course of iterations.

Therefore, in order to increase the convergence accuracy and efficiency and maintain a fine balance between global and local search mechanisms, following scheme given in Table 2 is designed and added the lines between 33 and 34. In Table 3, *Best* denotes the current global best result obtained from the iterations, *rand* is the Gaussian random number generated between 0 and 1. The

proposed scheme intends to enhance the convergence rate of the algorithm and avoids being trapped of the local optimum points in the search space. In order to assess the optimization performance of the propounded improved DS algorithm, eleven widely quoted optimization test functions (given in Table 4) are solved. Numerical results are benchmarked with those acquired by Differential Search (DS) [18], Bat algorithm (BAT) [31], Intelligent tuned Harmony Search (ITHS) [32], Big Bang – Big Crunch (BB-BC) [33] and Quantum behaved Particle Swarm Optimization (QPSO) [34,35]. For all benchmark functions, problem dimension is set to 30 and 40000 function evaluations are made.

**Table 3.** Proposed local search scheme procedure

```

for  $i = 1 : N$  do
     $X(i,:) = Stopoversite(i,:) - ((Stopoversite(i,:) - Best) \times rand_{11})$ 

```

```

 $Y(i,:) = Best + ((Stopoversite(i,:) - Best) \times rand_{12})$ 
endfor

for  $i = 1 : N$  do
    if  $Evaluate(X(i)) < Evaluate(Y(i))$  then
         $Stopoversite2(i,:) = X(i,:)$ 
    else
         $Stopoversite2(i,:) = Y(i,:)$ 
    endif
endfor

for  $i = 1 : N$  do
    if  $Evaluate(Stopoversite2(i)) < Evaluate(Stopoversite(i))$  then
         $Stopoversite(i,:) = Stopoversite2(i,:)$ 
    endif
endfor

```

**Table 4.** Formulations of the benchmark functions utilized in this study

|          | Function                                                                                                                                                                                                                                                                                                                                                  | D  | Range               | $f_{opt}$ |
|----------|-----------------------------------------------------------------------------------------------------------------------------------------------------------------------------------------------------------------------------------------------------------------------------------------------------------------------------------------------------------|----|---------------------|-----------|
| $f_1$    | Zakharov<br>$f_1(x) = \sum_{i=1}^D x_i^2 + \left( \sum_{i=1}^D 0.5ix_i \right)^2 + \left( \sum_{i=1}^D 0.5ix_i \right)^4$                                                                                                                                                                                                                                 | 30 | $[-5.0, 10.0]^D$    | 0         |
| $f_2$    | Sphere<br>$f_2(x) = \sum_{i=1}^D x_i^2$                                                                                                                                                                                                                                                                                                                   | 30 | $[-5.0, 5.0]^D$     | 0         |
| $f_3$    | Ackley<br>$f_3(x) = -20 \exp \left( -0.2 \sqrt{\frac{1}{D} \sum_{i=1}^D x_i^2} \right) - \exp \left( \frac{1}{D} \sum_{i=1}^D \cos(2.0\pi x_i) \right) + 20 + e$                                                                                                                                                                                          | 30 | $[-32.0, 32.0]^D$   | 0         |
| $f_4$    | Griewank<br>$f_4(x) = \frac{1}{4000} \sum_{i=1}^D x_i^2 - \prod_{i=1}^D \cos \left( \frac{x_i}{\sqrt{i}} \right) + 1$                                                                                                                                                                                                                                     | 30 | $[-600, 600]^D$     | 0         |
| $f_5$    | Levy<br>$f_5(x) = \sin^2(\pi w_1) + \sum_{i=1}^{D-1} (w_i - 1)^2 [1 + 10 \sin(\pi w_1 + 1)] + (w_D - 1)^2 [1 + \sin^2(2\pi w_D)]$<br>where $w_i = 1 + \frac{x_i - 1}{4}$ , for all $i = 1, \dots, D$                                                                                                                                                      | 30 | $[-50.0, 50.0]^D$   | 0         |
| $f_6$    | Penalized1<br>$f_6(x) = \frac{\pi}{D} \left\{ 10 \sin^2(\pi y_1) + \sum_{i=1}^{D-1} (y_i - 1)^2 [1 + 10 \sin^2(\pi y_{i+1})] + (y_D - 1)^2 \right\}$<br>$+ \sum_{i=1}^D u(x_i, 10, 100, 4)$<br>$u(x_i, a, k, m) = \begin{cases} k(x_i - a)^m, & x_i > a \\ 0, & -a \leq x_i \leq a \\ k(-x_i - a)^m, & x_i < -a \end{cases}$<br>$y_i = 1 + 0.25(x_i + 1)$ | 30 | $[-50.0, 50.0]^D$   | 0         |
| $f_7$    | Rastrigin<br>$f_7(x) = \sum_{i=1}^D (x_i^2 - 10 \cos(2.0\pi x_i)) + 10D$                                                                                                                                                                                                                                                                                  | 30 | $[-5.12, 5.12]^D$   | 0         |
| $f_8$    | Rosenbrock<br>$f_8(x) = \sum_{i=1}^{D-1} \left[ 100(x_{i+1} - x_i^2)^2 + (x_i - 1)^2 \right]$                                                                                                                                                                                                                                                             | 30 | $[-2.0, 2.0]^D$     | 0         |
| $f_9$    | Step<br>$f_9(x) = \sum_{i=0}^{D-1} (\lfloor x_i \rfloor + 0.5)^2$                                                                                                                                                                                                                                                                                         | 30 | $[-100.0, 100.0]^D$ | 0         |
| $f_{10}$ | Pathologic<br>$f_{10}(x) = \sum_{i=1}^{D-1} \left( 0.5 + \frac{\sin^2 \left( \sqrt{100x_i^2 + x_{i+1}^2} \right) - 0.5}{1 + 0.001(x_i^2 - 2x_i x_{i+1} + x_{i+1}^2)} \right)^2$                                                                                                                                                                           | 30 | $[-100.0, 100.0]^D$ | 0         |
| $f_{11}$ | Alpine<br>$f_{11}(x) = \sum_{i=1}^D  x_i \sin(x_i) + 0.1x_i $                                                                                                                                                                                                                                                                                             | 30 | $[-50.0, 50.0]^D$   | 0         |

50 consecutive algorithm runs are performed considering the stochastic nature of the aforementioned metaheuristic methods. Algorithms are developed in Java and run on Intel Core with 2.50 Ghz CPU and 6.0 GB RAM.

Each of these optimizers has algorithm specific tuning parameters to be used in perturbations. For QPSO algorithm, cognitive and social parameters are set to 2.0 and contraction-expansion coefficient which controls the convergent behavior of the

algorithm varies as iterations proceed. This value is initialized as  $w_i=1.0$  and descends to  $w_i=0.5$  on the course of iterations

**Table 5.** Comparison of the statistical results for each optimizer

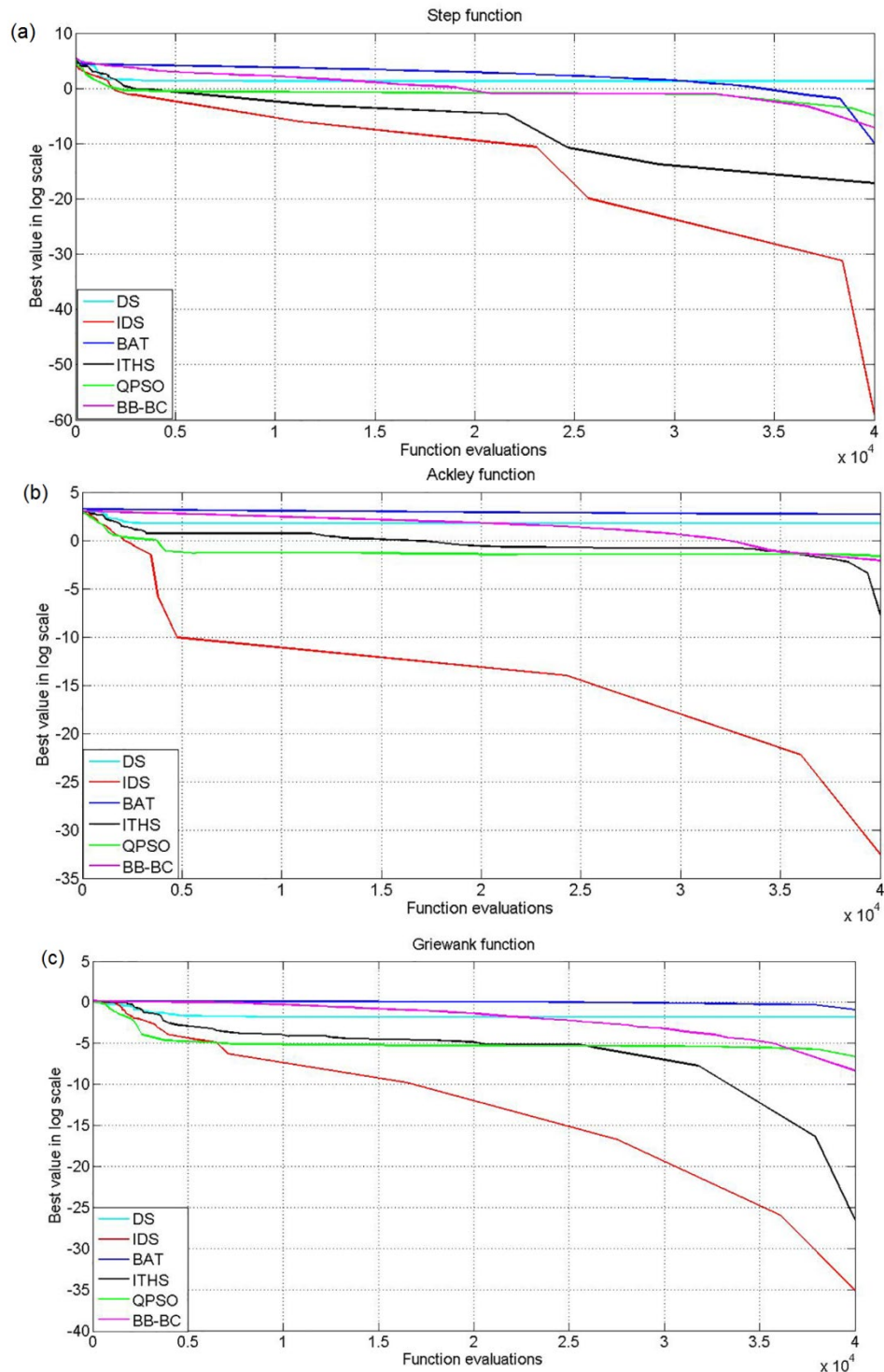
|                                  | Best            | Mean     | Std.dev. | Worst    |
|----------------------------------|-----------------|----------|----------|----------|
| <i>f<sub>1</sub></i> Zakharov    |                 |          |          |          |
| IDS                              | <b>4.88E-19</b> | 1.15E-15 | 4.43E-15 | 3.55E-14 |
| DS                               | 1.07E+01        | 3.06E+01 | 9.76E+00 | 5.06E+01 |
| BAT                              | 3.69E+01        | 2.28E+06 | 1.56E+07 | 1.30E+08 |
| ITHS                             | 2.14E-04        | 5.66E-01 | 1.04E+00 | 6.79E+00 |
| BB-BC                            | 2.15E+01        | 1.46E+02 | 7.42E+01 | 3.54E+02 |
| QPSO                             | 1.64E-01        | 5.65E+00 | 5.07E+00 | 1.97E+01 |
| <i>f<sub>2</sub></i> Sphere      |                 |          |          |          |
| IDS                              | <b>1.44E-26</b> | 1.33E-22 | 4.77E-22 | 2.70E-21 |
| DS                               | 3.44E+00        | 7.85E+00 | 2.04E+00 | 1.43E+01 |
| BAT                              | 2.78E-05        | 1.30E+01 | 8.18E+00 | 3.41E+01 |
| ITHS                             | 2.20E-10        | 2.50E-02 | 1.24E-01 | 1.12E-02 |
| BB-BC                            | 7.06E-04        | 1.07E-01 | 2.65E-01 | 1.27E+00 |
| QPSO                             | 3.34E-03        | 3.45E-01 | 6.24E-01 | 2.93E+00 |
| <i>f<sub>3</sub></i> Ackley      |                 |          |          |          |
| IDS                              | <b>7.54E-15</b> | 1.44E-14 | 9.02E-15 | 4.30E-14 |
| DS                               | 5.88E+00        | 8.62E+00 | 1.17E+00 | 1.20E+00 |
| BAT                              | 1.12E+01        | 1.97E+01 | 7.43E-01 | 2.07E+01 |
| ITHS                             | 4.30E-04        | 4.62E-01 | 4.42E-01 | 2.50E+00 |
| BB-BC                            | 1.23E-01        | 8.23E-01 | 1.42E+00 | 6.64E+00 |
| QPSO                             | 1.99E-01        | 1.72E+00 | 1.38E+00 | 5.95E+00 |
| <i>f<sub>4</sub></i> Griewank    |                 |          |          |          |
| IDS                              | <b>5.55E-16</b> | 1.16E-14 | 4.68E-15 | 2.17E-14 |
| DS                               | 1.66E-01        | 3.18E-01 | 7.96E-02 | 5.65E-01 |
| BAT                              | 3.98E-01        | 1.06E+00 | 3.17E-02 | 1.10E+00 |
| ITHS                             | 3.10E-12        | 2.22E-02 | 5.32E-02 | 3.27E-01 |
| BB-BC                            | 2.37E-04        | 3.63E-02 | 5.71E-02 | 3.76E-01 |
| QPSO                             | 1.34E-03        | 6.94E-02 | 1.09E-01 | 6.65E-01 |
| <i>f<sub>5</sub></i> Levy        |                 |          |          |          |
| IDS                              | 1.72E-01        | 4.42E+00 | 2.28E+00 | 9.97E+00 |
| DS                               | 4.23E+00        | 8.29E+00 | 2.82E+00 | 1.68E+01 |
| BAT                              | 1.06E+01        | 4.68E+01 | 2.07E+01 | 1.68E+02 |
| ITHS                             | <b>1.17E-06</b> | 5.68E-02 | 7.84E-02 | 2.85E-01 |
| BB-BC                            | 1.94E+01        | 3.78E+01 | 8.92E+00 | 5.54E+01 |
| QPSO                             | 1.00E+00        | 5.63E+00 | 3.19E+00 | 1.23E+01 |
| <i>f<sub>6</sub></i> Penalized1  |                 |          |          |          |
| IDS                              | <b>9.01E-11</b> | 9.01E-11 | 9.93E-22 | 9.01E-11 |
| DS                               | 1.34E-01        | 2.97E-01 | 1.13E-01 | 6.32E-01 |
| BAT                              | 2.83E-02        | 8.03E-01 | 3.45E-01 | 1.54E+00 |
| ITHS                             | 1.50E-07        | 3.56E-04 | 3.56E-04 | 3.34E-03 |
| BB-BC                            | 1.01E-01        | 8.29E-01 | 3.13E-01 | 1.63E+00 |
| QPSO                             | 5.83E-05        | 2.48E-02 | 4.22E-02 | 1.08E-01 |
| <i>f<sub>7</sub></i> Rastrigin   |                 |          |          |          |
| IDS                              | 1.79E+01        | 3.93E+01 | 1.06E+01 | 5.93E+01 |
| DS                               | 1.07E+02        | 1.54E+02 | 1.56E+01 | 1.88E+02 |
| BAT                              | 7.95E+01        | 2.05E+02 | 3.94E+01 | 2.70E+02 |
| ITHS                             | <b>1.30E-06</b> | 5.83E+01 | 2.54E+01 | 1.05E+02 |
| BB-BC                            | 1.17E+02        | 1.93E+02 | 3.54E+01 | 2.77E+02 |
| QPSO                             | 2.93E+01        | 5.61E+01 | 1.54E+01 | 9.93E+01 |
| <i>f<sub>8</sub></i> Rosenbrock  |                 |          |          |          |
| IDS                              | <b>1.33E+01</b> | 2.36E+01 | 2.54E+00 | 2.84E+01 |
| DS                               | 8.58E+01        | 1.57E+02 | 4.12E+01 | 2.79E+02 |
| BAT                              | 2.07E+01        | 2.93E+01 | 1.43E+01 | 8.54E+01 |
| ITHS                             | 2.84E+01        | 3.64E+01 | 2.54E+01 | 1.68E+02 |
| BB-BC                            | 2.47E+01        | 7.54E+01 | 3.88E+01 | 2.01E+02 |
| QPSO                             | 2.58E+01        | 7.13E+01 | 3.52E+01 | 1.71E+02 |
| <i>f<sub>9</sub></i> Step        |                 |          |          |          |
| IDS                              | <b>7.10E-26</b> | 1.27E-21 | 6.77E-21 | 4.82E-20 |
| DS                               | 3.66E+00        | 8.86E+00 | 2.67E+00 | 1.72E+01 |
| BAT                              | 5.17E-05        | 1.27E+01 | 6.46E+00 | 2.83E+01 |
| ITHS                             | 3.43E-08        | 2.41E-02 | 3.54E-02 | 1.66E-01 |
| BB-BC                            | 8.01E-04        | 3.15E-01 | 9.93E-01 | 6.29E+00 |
| QPSO                             | 7.24E-03        | 2.89E-01 | 3.72E-01 | 1.76E+00 |
| <i>f<sub>10</sub></i> Pathologic |                 |          |          |          |
| IDS                              | <b>2.17E-01</b> | 5.23E-01 | 2.62E-01 | 1.23E+00 |
| DS                               | 1.19E+00        | 2.59E+00 | 4.86E-01 | 3.43E+00 |
| BAT                              | 2.99E-01        | 5.61E-01 | 3.16E-01 | 1.83E+00 |
| ITHS                             | 5.61E-01        | 1.06E+00 | 3.14E-01 | 1.83E+00 |
| BB-BC                            | 1.20E+00        | 2.86E+00 | 7.51E-01 | 3.92E+00 |
| QPSO                             | 4.34E-01        | 2.12E+00 | 6.23E-01 | 3.49E+00 |
| <i>f<sub>11</sub></i> Alpine     |                 |          |          |          |
| IDS                              | <b>2.06E-15</b> | 1.48E-14 | 2.62E-14 | 1.17E-13 |
| DS                               | 8.57E+00        | 1.21E+01 | 1.65E+00 | 1.56E+01 |
| BAT                              | 9.34E+00        | 2.05E+01 | 7.33E+00 | 5.67E+01 |
| ITHS                             | 1.32E-05        | 1.98E-01 | 5.34E-01 | 4.41E+00 |
| BB-BC                            | 3.32E+00        | 9.19E+00 | 2.48E+00 | 1.94E+01 |
| QPSO                             | 2.11E-03        | 2.11E-01 | 2.23E-01 | 9.15E-01 |

Harmony memory consideration rate, responsible for decision of choosing decision variables from the harmony memory, is fixed to 0.95 for ITHS algorithm. Iteration dependent parameters including loudness and pulse emission rate are respectively set to 1.5 and 0.5.

for Bat algorithm. A parameter for limiting the size of the search space is set to 0.6 for BB-BC algorithm. Table 5 reports the comparison of the statistical results for the mentioned metaheuristic algorithms obtained after 50 algorithm runs. It is

clearly observed that proposed Improved DS algorithm (IDS) outperforms the compared optimizers in terms of statistical results it attains. Except for Levy and Rastrigin functions, which are dominated by the ITHS method with respect to obtained best results, IDS finds much better solutions and shows quick convergence after 40000 function evaluations as it is depicted in Fig 2(a-e). The convergence histories of these six algorithms are

explicitly given for four test functions including Ackley, Penalized1, Step, Griewank, and Levy in Fig 2(a-e). Evolution characteristic of the optimizers reveals that convergence performance of the proposed IDS is highly superior to the remaining algorithms (except for Levy function) since it reaches to minimum value faster than the others.





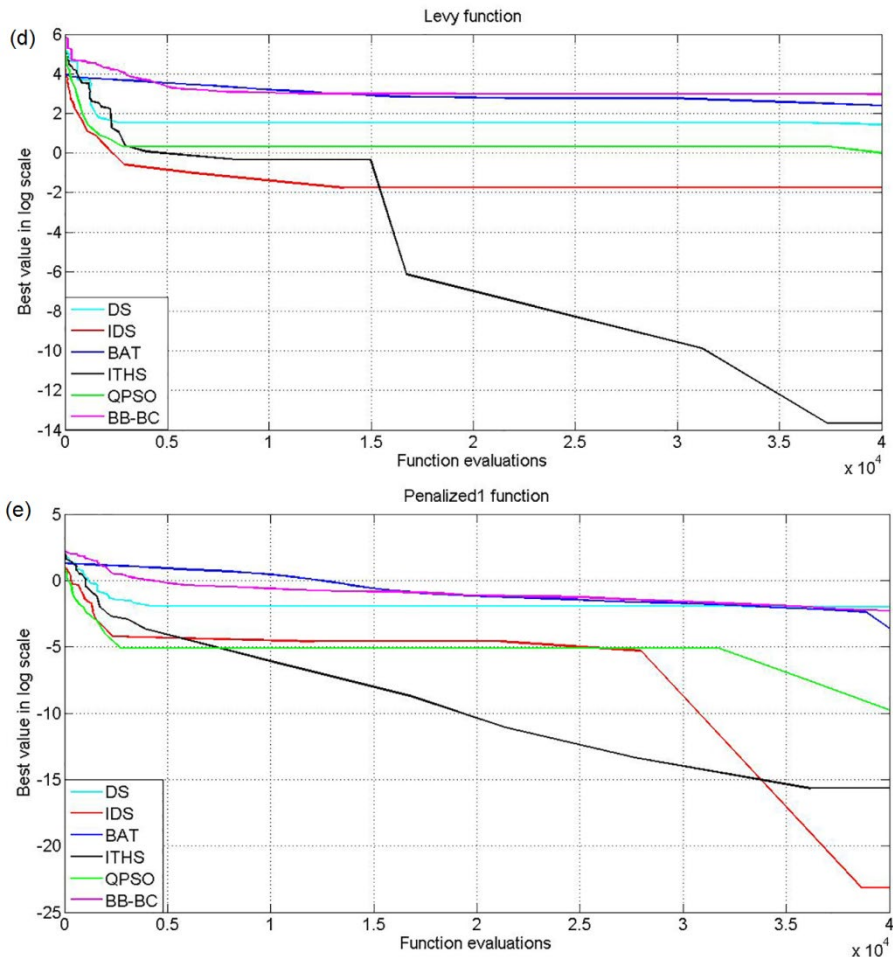


**Figure 2.** (a) Convergence histories of the optimization methods for Step function  
 (b) Evolution histories of the optimization methods for Ackley function  
 (c) Evolution process of the optimization methods for Griewank function  
 (d) Convergence process of the optimization methods for Levy function  
 (e) Convergence characteristics of the optimization methods for Penalized1 function

## Results and Discussion

In order to design plate fin heat sinks under the effect of two conflicting objectives with imposed constraints, Improved Differential Search algorithm is proposed in this paper. Problem at hand is a constrained engineering design problem so it should be converted into unconstrained problem by applying penalty function as described in the equations below

$$f_1 = \dot{S}_{gen} + P \times \left( \sum_{i=1}^5 G_i^*(\vec{x}) \right) \quad (26)$$

and

$$f_2 = C_{mat} + P \times \left( \sum_{i=1}^5 G_i^*(\vec{x}) \right) \quad (27)$$

Where  $G_i^* = \max(G_i, 0)$ ,  $P$  is the penalty coefficient that penalized the unfeasible solutions, and  $\vec{x} = \{W, L, H, t_b, t_w, V_f, N\}$  is the set of decision variables to be optimized. Penalty factor in Eqs (26) and (27) is a problem

dependent coefficient, which is a considerable high value and chosen by trial and error methodology. For this multi-objective design problem, this is set to 50000.

In thermal design of heat exchanger components, main aim is either to minimize the total thermal resistance or maximize thermal efficiency by enhancing heat transfer coefficient rates. In addition, it is also endeavored to reduce the total cost of the heat exchanger while satisfying consumer's needs. Design of a heat sink is a bit similar to this. When it is to consider plate fin heat sink design problem, the heat dissipation and the stream temperature can be specified in advance [36]. Therefore, it can be inferred, as plate fin heat sink design in terms of entropy generation minimization is somewhat similar to minimization of total thermal resistance on the connecting layers. In addition, optimum values of oncoming stream velocity and drag force coefficient have decisive effects on minimizing total entropy generation. Optimum design of plate fin heat sink with flow through and impingement-flow air cooling systems configuration is accomplished by the proposed DS algorithm in this paper. A case study taken from Chen and Chen [1] is used to test the performance of the IDS on real world optimization design problems. Seven design variables including oncoming stream velocity ( $V_f$ ), number of fins on the plate ( $N$ ), gap between consecutive fins ( $b$ ), base thickness of the plate ( $t_b$ ), Width ( $W$ ), Length ( $L$ ) and Height ( $H$ ) of the fins are selected in order to optimize above given objectives simultaneously. Table 6 reports

the operating conditions and corresponding physical parameters of the plate heat sink. The task is to determine optimal configuration of plate fin heat sink under given conditions for both flow patterns. Fig 3 shows the concurrent optimization results concerning minimum cost of the material and entropy generation for flow-through configuration. Fig. 3 declares that there are three optimal solution found by three different decision making theories. In multi objective optimization, decision making plays important role in selection of optimal solutions from the pareto frontier. Several methods can be found in literature for decision-making process. TOPSIS, LINMAP and Shannon's entropy approach, which are also utilized in this study, are the most prevalent ones among of all methods. For fair comparison between the results retained from three methods, the deviation index term comes into practice to evaluate the discrepancies among three solutions. In terms of numerical analysis, lower value of deviation index indicates its closeness to the ideal point.

**Table 6.** Operation conditions and design parameters of the heat sink system

| Parameters or conditions      | Unit              | Value  |
|-------------------------------|-------------------|--------|
| Thermal conductivity of solid | W/mK              | 200    |
| Thermal conductivity of air   | W/mK              | 0.0267 |
| Density of solid (fin)        | kg/m <sup>3</sup> | 2707   |
| Density of air                | kg/m <sup>3</sup> | 1.177  |
| Kinematic viscosity of air    | m <sup>2</sup> /s | 1.6e-5 |
| Prandtl number of air         | -                 | 0.703  |
| Heat load                     | W                 | 30     |
| Ambient temperature           | K                 | 298    |
| Price of aluminum             | NTD/kg            | 65     |

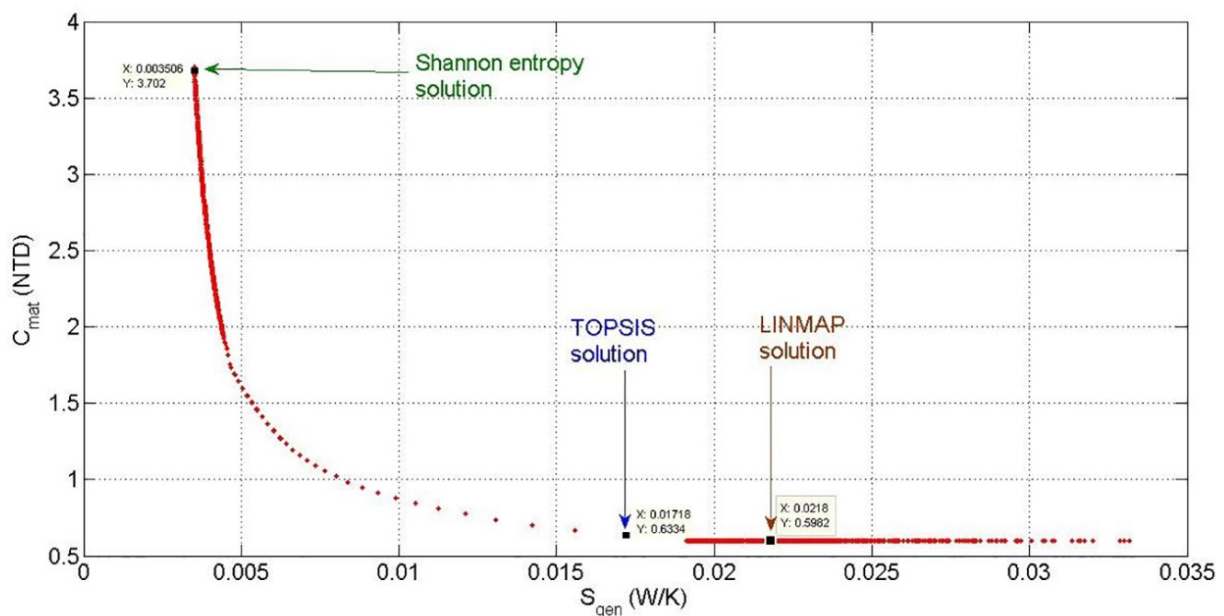


**Figure 3.** Pareto optimum solutions for flow through configuration

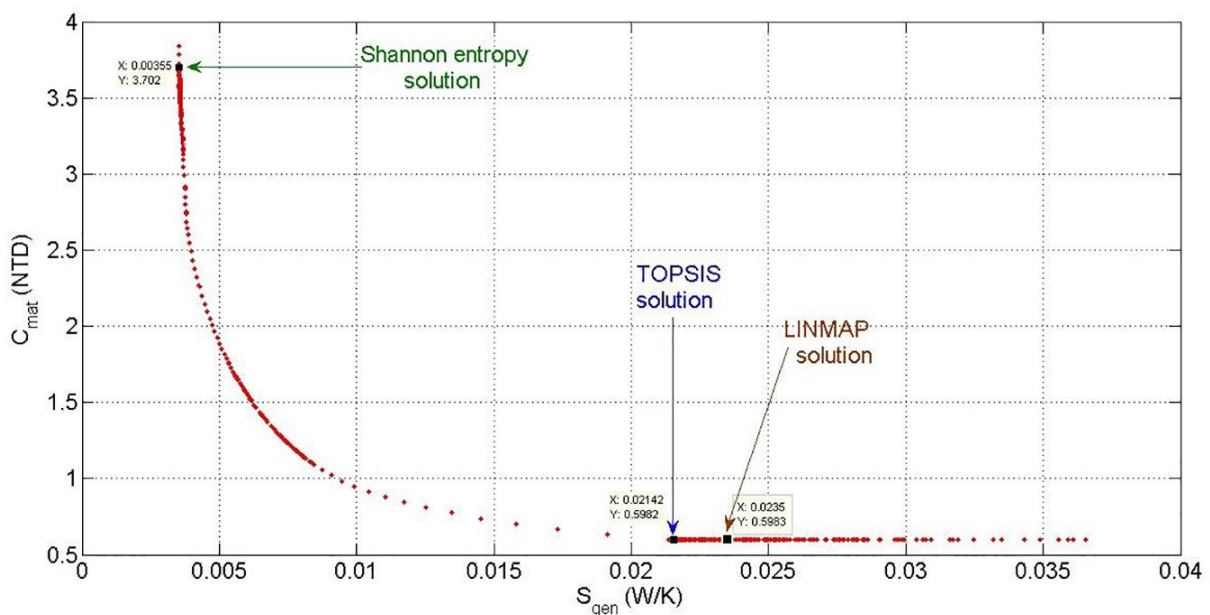


**Figure 4.** Pareto optimum solutions for impingement flow configuration

**Table 7. Optimum solutions for flow through configuration**

| Decision making methods                                | Optimization variables |        |                     |        |        |                      |    |        | Objectives             |                        | Deviation index |
|--------------------------------------------------------|------------------------|--------|---------------------|--------|--------|----------------------|----|--------|------------------------|------------------------|-----------------|
|                                                        | W (mm)                 | L (mm) | t <sub>b</sub> (mm) | H (mm) | b (mm) | V <sub>f</sub> (m/s) | N  | t (mm) | S <sub>gen</sub> (W/K) | C <sub>mat</sub> (NTD) |                 |
| TOPSIS                                                 | 40.000                 | 40.000 | 1.000               | 25.000 | 4.222  | 2.444                | 10 | 0.200  | 0.01718                | 0.63341                | 0.0273          |
| LINMAP                                                 | 40.000                 | 40.000 | 1.000               | 25.000 | 4.775  | 1.698                | 9  | 0.200  | 0.02184                | 0.59824                | 0.5101          |
| Shannon's entropy theory                               | 59.747                 | 59.999 | 1.000               | 26.211 | 1.352  | 2.499                | 37 | 0.300  | 0.00350                | 3.70281                | 0.0231          |
| Single objective concerning minimum entropy generation | 59.745                 | 59.997 | 1.002               | 26.213 | 1.351  | 2.499                | 37 | 0.299  | 0.003507               | 3.70367                |                 |
| Single objective concerning minimum material cost      | 40.000                 | 40.000 | 1.000               | 25.000 | 5.485  | 1.909                | 8  | 0.200  | 0.02353                | 0.59824                |                 |

**Table 8. Optimum solutions for impingement flow configuration**

| Decision making methods                                | Optimization variables |        |                     |        |        |                      |    |        | Objectives             |                        | Deviation index |
|--------------------------------------------------------|------------------------|--------|---------------------|--------|--------|----------------------|----|--------|------------------------|------------------------|-----------------|
|                                                        | W (mm)                 | L (mm) | t <sub>b</sub> (mm) | H (mm) | b (mm) | V <sub>f</sub> (m/s) | N  | t (mm) | S <sub>gen</sub> (W/K) | C <sub>mat</sub> (NTD) |                 |
| TOPSIS                                                 | 40.000                 | 40.000 | 1.000               | 25.000 | 4.777  | 2.492                | 9  | 0.200  | 0.02142                | 0.59825                | 0.0604          |
| LINMAP                                                 | 40.000                 | 40.000 | 1.000               | 25.000 | 4.771  | 1.944                | 9  | 0.200  | 0.02353                | 0.59825                | 0.5240          |
| Shannon's entropy theory                               | 59.999                 | 59.999 | 1.111               | 25.000 | 1.312  | 1.999                | 38 | 0.299  | 0.00355                | 3.70211                | 0.0501          |
| Single objective concerning minimum entropy generation | 59.995                 | 60.000 | 1.597               | 25.000 | 1.313  | 2.497                | 38 | 2.991  | 0.00355                | 4.02097                |                 |
| Single objective concerning minimum material cost      | 40.000                 | 40.000 | 1.000               | 25.000 | 4.775  | 1.533                | 9  | 2.000  | 0.02501                | 0.59824                |                 |

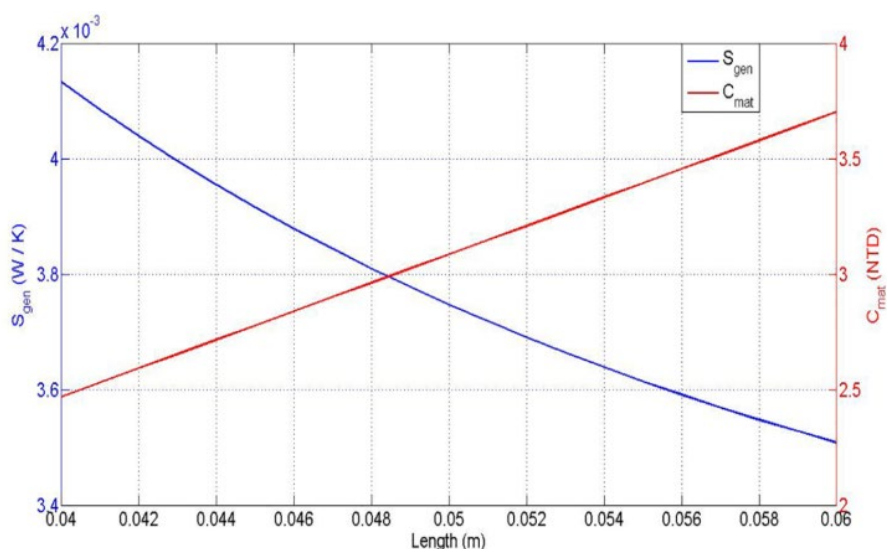


**Figure 5. Influences of plate fin heat sink length on total entropy generation and material cost values**

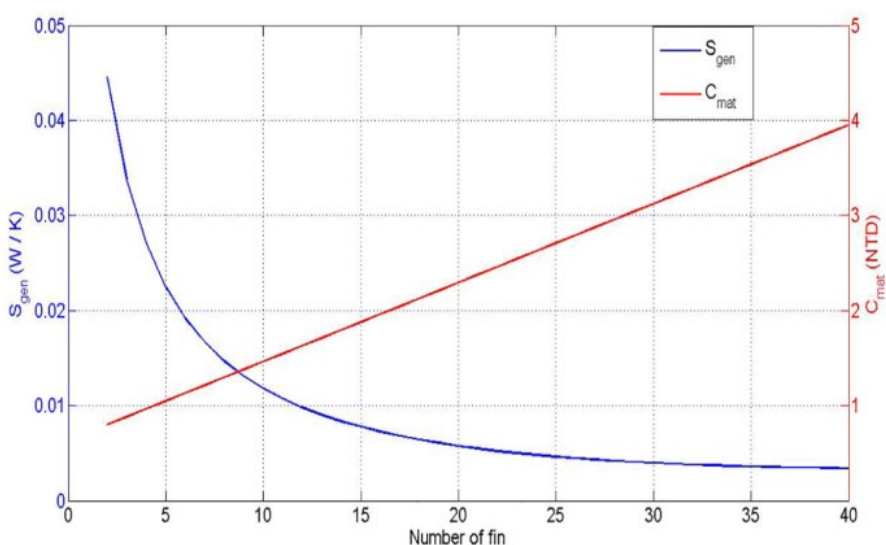


**Figure 6. Effects of fin numbers on the plate over total entropy generation and material cost values**

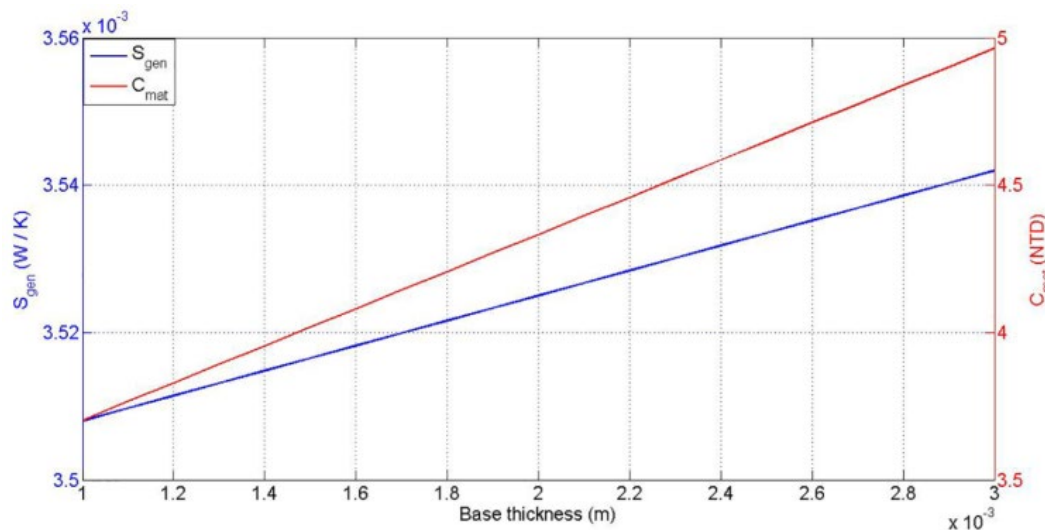


Figure 7. Influences of base thickness rates on total entropy generation and material cost values

For this reason, utilization of deviation index factor gives tangible ideas as to which decision making theory is suitable for that particular case. To summarize, lesser value it attains more reliable technique is for that case. Description and formulation of these methodologies are not given in this paper however, interested readers can find the detailed explanation about these methods in [37,38]. According to the results found by these decision making theories, optimal solution reached by TOPSIS and LINMAP inclined towards higher values of entropy generation while the solution found by Shannon's entropy theory lies on higher material cost side of the pareto frontier. Table 7 reports the optimal solutions for three decision methods along with their corresponding deviation indexes for flow through configuration. Shannon's entropy method yields lower value of deviation index of 0.0231 while LINMAP and TOPSIS are respectively having that value of 0.5101 and 0.0273. It can be concluded that result on the pareto frontier found by Shannon's entropy approach is more reliable than that of the others. Table 7 also reports the single optimization results concerning minimum entropy generation and minimum cost of material. Minimum solution obtained for entropy generation is 0.003507 W/K while minimum total cost value for this case is found to be 0.59824 NTD. Algorithm pushes the decision variables of heat sink plate weight, length and height into their lower boundaries when considering total cost minimization. On the contrary, these aforementioned decision variables get their maximum values, and in addition to this, number of fins shows tendencies to increase when minimum entropy generation rate is on the process. It is what expected from the algorithm since as fin numbers increases to given extent in Table 7, a marked rise is seen in total heat transfer area and correspondingly total heat resistance reduces which leads to significant decrease in total entropy generation rates. Fig. 4 presents the pareto frontier for plate fin heat sink equipped with impingement air cooling system. It is observed from the figure that TOPSIS and LINMAP decision-making theories are prone to get the trade-off results from the x-axis ( $S_{gen}$ ) while the outcomes of Shannon's entropy theory are inclined to y-axis ( $C_{mat}$ ). Table 8 gives the optimal solutions gathered by different decision-making methods along with respective deviation indexes as well as the results of the single objective optimization cases for impingement flow configuration. As it seen from the deviation index values, Shannon's entropy theory is the most reliable one among three decision making methods. And also, it is observed that the results obtained for impingement flow configuration are similar with those retained for flow-through configuration in terms of the numerical behaviors of the decision variables. Fig. 5 to 7 shows the behaviors of the objective functions as some of optimization variables switch their lower to upper

bounds for flow-through configuration. Fig. 5 depicts the inclinations of two objectives as length of heat sink plate varies. It is shown that total entropy generation decreases while total cost increase as plate length increases. Fig. 6 shows the variation of the two conflicting objectives as number of the fins on the plate increases. Total cost of materials goes up while a parabolic decrease is seen as number of fins increases. As number of fins increase, total heat resistance will decrease due to reduction in denominator values in Eq.(2) for both flow configuration. This decline results in a decrease in entropy generation rates while causing a linear increase in total cost of materials because of the increment in total fin area. Fig. 7 visualizes the change in entropy generation and total material cost as thickness of the plate varies. Increase in entropy generation rates can be accounted for the increment in nominator of Eq (2).

## Conclusion

In the present work, improved Differential Search algorithm is developed to overcome the convergence deficiencies inherent in Differential Search algorithm. Differential Search simulates the migration behavior of the individuals on seeking of productive areas for subsistence. Local search based perturbation scheme is added into the proposed method in order to increase the solution accuracy and convergence speed of the algorithm. Effectiveness of the propounded method is tested on widely known optimization test functions and benchmarked against optimization methods including intelligent tuned Harmony Search, Big Bang- Big Crunch algorithm, Quantum behaved Particle Swarm Optimization, and Bat algorithm. Improved algorithm surpasses the compared optimizers for most cases and conquers some drawbacks with respect to convergence limitations. Performance of the upgraded method is then applied on multi-objective optimization of a plate-fin equipped with flow-through and impingement-flow air cooling system. The pareto front of multi-objective design is well located and gives good distribution all along the curve. Three different decision making approaches such as TOPSIS, LINMAP and Shannon's entropy theory are put into practice to decide the most reliable solution on the frontier. According to the corresponding deviation index values, method of Shannon's entropy theory gives the best trade-off solution between two objective functions for both flow configurations. Overall, under given operating conditions multi-objective design of the presented strategy yields to economical structural size while dissipating considerable amount of heat by means of simultaneous minimization of entropy generation rate and total cost of heat sink material.

## References

- [1] C.T. Chen, H.I. Chen, "Multi objective optimization design of plate-fin heat sinks using a direction-based genetic algorithm," *J. Taiwan Inst. Chem.*, vol.44, pp.257 – 265, 2013
- [2] A.D. Kraus, A. Bar-Cohen, "Design and analysis of heat sinks", Wiley, New York, 1995.
- [3] J.R. Culham, Y.S. Muzychka, "Optimization of plate fin heat sinks using entropy generation minimization," *IEEE T. Compon. Pack T.*, vol. 24, pp. 159 – 165, 2001.
- [4] E.M. Sparrow, B.R., Baliga, and S.V. Patankar, "Forced convection heat transfer from a shrouded fin arrays with and without tip clearance," *J. Heat Trans T. ASME*, vol.100, pp.572-579, 1978.
- [5] N. Goldberg, "Narrow channel forces air heat sink," *IEEE Trans. Compon. Packag. Manuf. Tech.*, vol.7, pp.154-159, 1984
- [6] R.W. Knight, J.S. Goodling, D.J. Hall, "Optimal thermal design of forced convection heat sinks- Analytical". *J Electron Packaging*, vol.113, pp.313-321, 1991.
- [7] R.W. Knight, J.S. Goodling, Gross. B.E. "Optimal thermal design of air-cooled forced convection finned heat sinks – Experimental verification," *IEEE Trans. Compon. Packag. Manuf. Tech.*, vol.15, pp.754-760, 1992.
- [8] A. Bejan, "Entropy generation through heat and fluid flow," Wiley, New York, 1982.
- [9] W.A. Khan, J.R. Culham, M.M. Yovanovich, "Optimization of pin-fin heat sinks using entropy generation minimization," *IEEE Trans. Compon. Packag. Manuf. Tech.*, vol.28, pp.247-254, 2005
- [10] S. Ndao, Y. Peles, M.K. Jensen, "Multi-objective thermal design optimization and comparative analysis of electronic cooling technologies," *Int. J. Heat Mass Transf.*, vol. 52, pp.4317- 4326, 2009
- [11] M.Iyengar, A. Bar-Cohen, "Least-energy optimization of forced convection plate-fin heat sinks," *IEEE T. Compon. Pack T.*, vol.26, pp.62-70, 2003
- [12] A. Bejan, A.M. Morega, "Optimal arrays of pin fins and plate fins in laminar forced convection," *J. Heat Trans T. ASME*, vol.115, pp.75-81, 1993
- [13] I.K. Karathanassis, E. Papanicolaou, V. Belessiotis, G.C. Bergeles, "Multi-objective design optimization of a micro heat sink for Concentrating Photovoltaic/Thermal (CPVT) systems using a genetic algorithm," *Appl. Therm. Eng.* vol.59, pp.733-744, 2013
- [14] R. Baby, C. Balaji, "Thermal optimization of PCM based pin fin heat sinks: An experimental study," *Appl. Therm. Eng.* vol.54, pp.65-77, 2013
- [15] D.K. Kim, "Thermal optimization of plate-fin heat sinks with fins of variable thickness under natural convection," *Int. J. Heat Mass Transfer*, vol.55, pp.752 – 761, 2012.
- [16] S. Soleimani, D.D. Ganji, M. Gorji, H. Baramia, E. Ghasemi, "Optimal location of a pair heat source-sink in an closed square cavity with natural convection through PSO algorithm," *Int. Commun. Heat Mass*, vol.38, pp.652 – 658, 2011
- [17] R.V. Rao, G.G. Waghmare, "Multi-objective design optimization of a plate-fin heat sink using a teaching-learning-based optimization algorithm," *Appl. Therm. Eng.*, vol. 76, pp. 521-529, 2015
- [18] P. Civicioglu, "Transforming geocentric cartesian coordinates to geodetic coordinates by using differential search algorithm," *Comput. Geosci.*, vol.46, pp.229 – 247, 2012.
- [19] M.A. Sahman, A.A. Altun, A. O. Dündar, "The Binary Differential Search Algorithm Approach for Solving Uncapacitated Facility Location Problems," *J. Comput. & Theo. Nanosci.*, vol.14, pp.670-684, 2017.
- [20] S. Ray, A. Bhattacharya, S. Bhattacharjee, "Differential Search Algorithm for Reliability Enhancement of Radial Distribution System," *Elec. Pow. Comp. & Syst.*, vol.44, pp.29-42, 2015.
- [21] V. Kumar, J.K. Chhabra, D. Kumar, "Differential Search Algorithm for Multiobjective Problems," *Proc. Comp. Sci.*, vol.48, pp.22 – 28, 2015.
- [22] A. Bejan, *Entropy generation minimization*. FL, CRC, Orlando, 1996
- [23] W.M. Kay, A.I. London, *Compact heat exchangers*, NewYork, McGraw-Hill, 1984
- [24] Y.S. Muzychka, M.M. Yovanovich, "Modeling friction factors in non-circular ducts for developing laminar flow," In: *Proceedings of 2<sup>nd</sup> AIAA Theoretical Fluid Mech. Meeting*, pp.15-28. 1998
- [25] F.M. White, *Fluid mechanics*, New York, McGraw-Hill, 1987
- [26] P.M. Teertstra, M.M. Yovanovich, J.R. Culham, T.F. Lemczyk, "Analytical forced convection modelling of plate fin heat sinks," In: *Proceedings of the 15<sup>th</sup> Annu. IEEE. Semicon. Therm. Meas. Manag. Symp.* pp.34-41, 1999.
- [27] J. Kennedy, R. Eberhart, "Particle swarm optimization," In: *Proceedings of IEEE International Conference on Neural Networks*. pp. 1942-1948, 1995.
- [28] D. Karaboga, "An idea based on honey bee swarm for numerical optimization," *Technical Report-TR06*, Erciyes University, Engineering Faculty, Computer Engineering Department, 2005
- [29] T. Vito, T. Elio, M.P. Kevin, A.R.M James, "Swarm cognition: an interdisciplinary approach to the study of self-organizing biological collectives," *Swarm Intell.*, vol.5, pp. 3-18, 2011
- [30] X.S. Yang, "Engineering optimization: an introduction with metaheuristic applications," John Wiley and Sons, USA, 2010.
- [31] X.S. Yang, "A new metaheuristic bat-inspired algorithm," In: J.R. Gonzalez et al. (Eds.) *Nature Inspired Cooperative Strategies for Optimization (NISCO 2010)*, *Studies in Computational Intelligence*, 284, Springer, Berlin, pp.65-74, 2010.
- [32] P. Yadav, R. Kumar, S.K. Panda, C.S. Chang, "An intelligent tuned harmony search algorithm for optimization," *Inform Sciences*, vol.196, pp.47-72, 2009
- [33] O.K. Erol, I. Eksin, "A new optimization method: Big Bang – Big Crunch," *Adv. Eng. Softw.*, vol. 37, pp. 106 – 111, 2006.
- [34] J. Sun, B. Feng, W. Xu, "Particle swarm optimization with particles having quantum behaviour," In: *Proceedings of the congress on evolutionary computation*. Portland, OR, USA, pp. 325- 331, 2004.
- [35] J. Sun, W. Xu, B. Feng, "Adaptive parameter control for quantum behaved particle swarm optimization on individual level," In: *Proceedings of IEEE International Conference on Systems, Man and Cybernetics, Big Islands, HI, USA*, pp. 3049 – 3054, 2005.
- [36] C.T. Chen, C.K. Wu, C. Hwang, "Optimal design and control of CPU heat sink processes." *IEEE Trans. Compon. Packag. Manuf. Tech.*, vol. 31, pp.184-195, 2008.
- [37] M.H. Ahmadi, H. Sayyadi, S. Dehghani, H. Hosseinz, "Design a solar powered Stirling heat engine load on multiple criteria: Maximized thermal efficiency and power," *Energy Convers. Manage.*, vol.75, pp. 282-291, 2013.
- [38] R. Arora, S.C. Kaushik, R. Kumar, R. Arora, "Multi-objective thermo-economic optimization of solar parabolic dish Stirling heat engine with regenerative losses using NSGA-II and decision making," *Int. J. Elec Power*, vol. 74, pp.25-35, 2016.